

In Situ Synthesis, Characterization of SiPMo-X, and Different Catalytic Properties of SiPMo-X and SiPW-X

Chunfeng Shi,^[a,bl] Runwei Wang,^{*[a]} Guangshan Zhu,^[a] Shilun Qiu,^{*[a]} and Jun Long^[bl]

Keywords: In situ synthesis / Heteropolyacids / Mesoporous materials / Encapsulation / Bulky molecule reactions / Zeolites

SBA-15 frameworks with encapsulated Keggin type heteropolyacids (HPAs) were synthesized in situ under strongly acidic conditions ($\text{pH} < 0$). During the hydrolysis of tetraethyl orthosilicate (TEOS), a P- and a Mo source were added into the initial sol-gel system to form Keggin type HPAs. The texture of the final products was studied by the N_2 adsorption-desorption isotherms and transmission electron microscopy (TEM), and their structure was systematically characterized by X-ray diffraction (XRD), UV/Vis diffuse reflectance (DRS), infrared- (IR), and ^{31}P magic angle spinning nuclear magnetic resonance (MAS NMR) spectroscopy. Characterization results suggest that the samples show very ordered hexagonal mesostructure, and the HPAs that are incorporated into the framework of meso-silica are insoluble during

catalysis. Results of catalytic tests indicate that the materials demonstrated catalytic activity comparable with or even surpassing those of the bulk HPAs in catalytic tests implementing chemical reactions of bulky molecules (1,3,5-triisopropylbenzene cracking, esterification of benzoic acid with *tert*-butyl alcohol, and 2,3,6-trimethylphenol hydroxylation with H_2O_2). Additionally, some other properties, such as easy separation and stability when recycled, ensure their potential applications in the chemical industries. Here, we report not only the in situ synthesis and characterization of SiPMo-X, but also the difference in the catalytic properties of SiPMo-X and SiPW-X.

(© Wiley-VCH Verlag GmbH & Co. KGaA, 69451 Weinheim, Germany, 2006)

Introduction

In recent years, environmental and economic considerations have raised strong interest in the redesign of commercially important processes so that the use of harmful substances and the generation of toxic wastes could be avoided. In this respect, there is no doubt that heterogeneous catalysis, as an alternative to homogeneous catalysis, can play a key role in the development of environmentally benign processes both in petroleum chemistry and in the production of chemicals, for example, by substitution of liquid acid catalysts by solid materials.^[1]

Most notably, zeolites and heteropoly compounds have attracted much attention not only as such acidic catalysts, but also as oxidation catalysts. First of all, zeolites, owing to their uniform intracrystalline microporosity that provides access to a very large and well-defined surface, the molecular sieve effect, and the strong electrostatic field centered at zeolite cations, promised unique opportunities from the

start for important improvements in efficiency and economy in gas and liquid sorption and separation technologies. The unique catalytic sites can catalyze many reactions, but zeolites also have some restrictions in general applications, such as weaker acidity, lack of variability in pore size, and the limited number of the constituent elements.^[2–12] For heteropoly compounds, peculiarly for HPAs, because their unique acidic and redox properties can be controlled at the atomic/molecular level, their catalytic function in the solid state as well as in solution has attracted much attention: the strong acidity or oxidizing properties of heteropoly compounds, the soft basicity of the polyanions, the high solubility in water and organic solvents, a moderately high thermal stability in the solid state, the relatively simple synthetic procedure, the ability to form pseudoliquid phases, and the possibility of the introduction of several different elements into polyanions and counter-cations. All the above-mentioned advantages of HPAs have led to a large body of work on their applications in homogeneous and heterogeneous catalysis.^[3–19] Soluble heteropoly compound catalysts (HPAs are typically strong Brønsted acids and are very soluble in oxygen-containing polar solvents such as water, alcohols, ethers, and ketones.) can catalyze a large variety of reaction types but suffer from their inability to be recycled.^[5–25] Much effort has been put into developing stable, water-tolerant solid acid catalysts, as such catalysts do not require a catalyst separation process after usage and are therefore much easier to use when compared with homo-

[a] State Key Laboratory of Inorganic Synthesis and Preparative Chemistry, Department of Chemistry, Jilin University, Changchun 130012, P. R. China
Fax: +86-431-5168589
E-mail: rwwang@mail.jlu.edu.cn
sjiu@mail.jlu.edu.cn

[b] Research Institute of Petroleum Processing, China Petroleum & Chemical Corporation (SINOPEC), Beijing 100083, P. R. China
Fax: +86-10-62311290
E-mail: shicf@ripp-sinopec.com

geneous acid catalysts. One approach to obtaining such a catalyst is to immobilize an active acidic species onto a solid support and to practically use this as a solid acidic catalyst. Moreover, the specific surface areas of solid HPAs are low (usually less than 10 m²/g), leading to very few active sites on their surfaces. Thus, immobilization of HPAs onto stable solid supports to create hybrid catalysts is absolutely necessary for using HPAs as solid catalysts. At the same time, their catalytic activities are expected to be improved by this procedure.^[10–28]

Mesoporous materials have attracted much attention because of their wide potential industrial applications as catalysts or catalyst supports and hosts since their discovery in the last decade, and it has been widely reported that mesoporous silica SBA-15 has been extensively used as a support and host because of its large pore size, thick walls, and high hydrothermal stability, which make it an excellent candidate for use as a stable solid support as mentioned above.^[29–40]

In our previous work, we prepared a series of insoluble HPA-containing hybrid catalysts by incorporation of HPAs into mesoporous supports during the formation of a mesostructure through acid-base interactions or covalent bond formation.^[23,25] We also investigated the heterogeneous catalytic behavior of these supported HPA catalysts in polar solvents. It was found that the catalytic activity of HPAs in the hybrid catalyst was significantly improved by the fascinating physical and chemical properties and the unusual internal surface topology of the mesoporous materials. Moreover, the separation and recovery of the HPAs from the reaction environment became easy.^[10,21,23,25] We also presented an in situ synthetic method for incorporating HPAs directly into the framework of mesoporous materials without destruction of the mesostructure. For example, we introduced Na₂HPO₄ and Na₂WO₄ (a P and a W source) or H₃PO₄ and Na₂MoO₄ (a P and an Mo source) into the initial sol-gel during the preparation of SBA-15 and successfully synthesized in situ new mesoporous silica encapsulated with Keggin type HPAs. Here we report not only the in situ synthesis and characterization of SiPMo-X, but also the different catalytic properties of SiPMo-X and SiPW-X.

Results and Discussion

Spectroscopy

X-ray Diffraction

Low-angle powder XRD patterns of SiPMo-8, HPMo/SBA, and SBA-15 samples are shown in Figure 1. Obvi-

ously, the sample of SiPMo-8 (Figure 1b and Table 1) exhibits three clearly well-resolved peaks indexed as (100), (110), and (200), which may be associated with the *p6mm* hexagonal symmetry similar to that of pure silica SBA-15 (Figure 1a).^[32] The three clearly well-resolved peaks may also indicate that SiPMo-8 is characterized by the presence of long-range ordering and that the ordering of SiPMo-8 may also be comparable to that of SBA-15. These results indicate that the formation and presence of HPMo in the framework of SBA-15, by the addition of H₃PO₄ and Na₂MoO₄ into the sol-gel during the hydrolysis of TEOS, does not affect the formation of the mesoporous structure of SBA-15. However, the ordering of conventionally supported HPMo (SBA-15 as the support) (Figure 1c) decreases significantly compared with that of SBA-15, which may be attributed to the fact that the conventional preparation method affects the ordering of the support. Moreover, from Figure 2, we can see that the wide-angle powder XRD

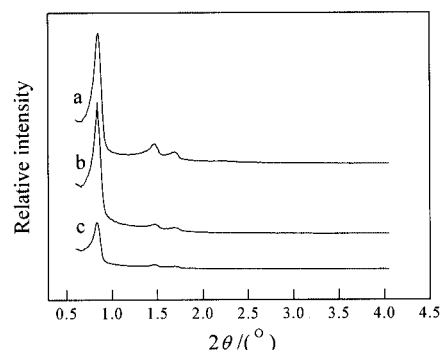


Figure 1. Small-angle XRD patterns of samples: (a) SBA-15, (b) SiPMo-8, and (c) HPMo/SBA.

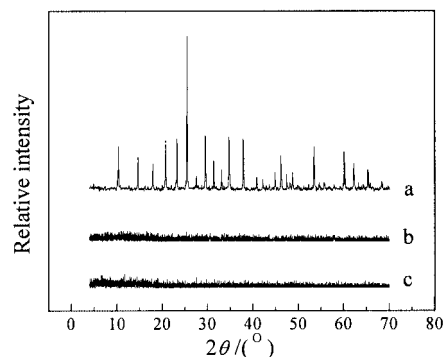


Figure 2. Wide-angle XRD patterns of samples: (a) HPMo, (b) SiPMo-8, and (c) HPMo/SBA.

Table 1. HPMo content and parameters of the pore structure of SiPMo-8, SBA-15, HPMo, and HPMo/SBA.

Samples	HPW content (wt.-%)		$d_{(100)}$ [nm]	a [nm]	Pore size [nm]	Wall thickness [nm] ^[a]	Surface area [m ² /g]	Pore volume [cm ³ /g]	Carbon residue ^[b]
	Sol-gel	Product							
SiPMo-8	33.3	19.6	10.4	12.0	7.6	4.4	807	1.04	10.9
SBA-15	0.0	0.0	10.3	11.9	7.9	4.0	860	1.15	8.8
HPMo/SBA	20.0	20.0	10.3	11.9	7.8	4.1	473	0.85	8.2
HPMo	100	100	–	–	–	–	5	–	–

[a] Pore size distributions were determined from N₂ adsorption isotherms and the wall thickness was calculated as: thickness = $a - \text{pore size}$ ($a = 2 \times d_{(100)}/3^{1/2}$). [b] The units for the carbon residue of samples are $\times 10^{-6}$ mmol/g.

patterns of SiPMo-8 (Figure 2b) do not show any obvious characteristic signals for pure HPMo, indicating the very high dispersion of HPMo in the meso-silica matrix.^[17,23,25,35]

Transmission Electron Microscopy

Figure 3 shows the TEM images of SiPMo-8 and SBA-15; we can see that the pores of the modified sample SiPMo-8 (Figure 3a, b) represent a hexagonal analogue to that of pure silica SBA-15 (Figure 3c, d).^[32] Compared with Figure 3c, d, the images shown in Figure 3a, b suggest that the ordering of the sample SiPMo-8 is only slightly less than that of the SBA-15 sample; these results are consistent with those from XRD.

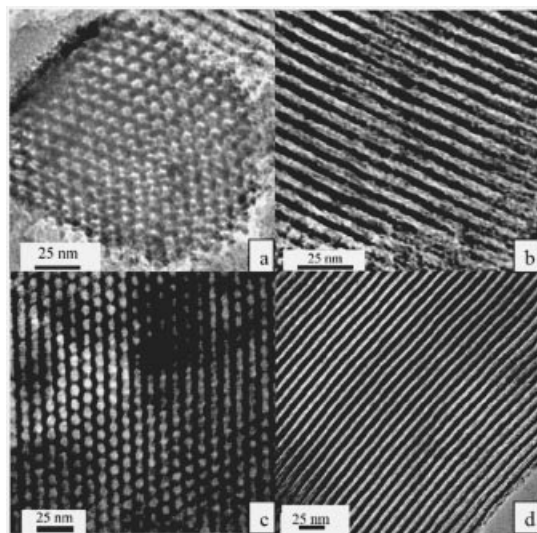


Figure 3. TEM images of samples: (a) SiPMo-8 in the [100] direction, (b) SiPMo-8 in the [110] direction, (c) SBA-15 in the [100] direction, and (d) SBA-15 in the [110] direction.

N₂ Adsorption Isotherms

The N₂ adsorption isotherms of the SiPMo-8 and HPMo/SBA samples together with that of pure silica SBA-15 are shown in Figure 4, and the porosity parameters, such as the BET specific area, cumulative pore volume, and average pore diameter, are listed in Table 1. Evidently, SiPMo-8 shows a typical adsorption curve of type IV (according to the IUPAC classification) with an obvious hysteresis loop at a relative pressure of $0.70 < P/P_0 < 0.85$ (Figure 4b) that is very similar to that of pure silica SBA-15 (Figure 4a).^[32] The hysteresis loop for the material starting at about 0.70 relative pressure suggests the presence of framework mesoporosity. In situ incorporation of HPMo into the framework of SBA-15 only leads to a very slight decrease in the values of surface area and pore volume. For example, the BET surface area and pore volume of SiPMo-8 are given as 807 m²/g and 1.04 cm³/g, and the corresponding values for SBA-15 are 860 m²/g and 1.15 cm³/g, so there is no clear difference between the porosity parameters of pure silica SBA-15 and the SiPMo-8 sample, implying the formation and presence of HPMo in the initial gel does not

affect the formation of a mesostructure, which is also in agreement with the XRD results. However, the BET surface area and pore volume of HPMo/SBA (Figure 4c) are 473 m²/g and 0.85 cm³/g, respectively, and comparing these results with the corresponding values for pure silica SBA-15, the BET surface area and pore volume of HPMo/SBA are significantly lower; these results also provide evidence that the conventional preparation method affects the ordering of the support.

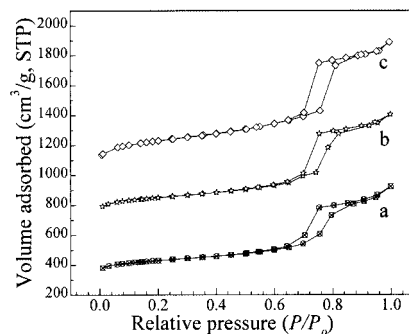


Figure 4. N₂ adsorption/desorption isotherms of samples at STP: (a) HPMo/SBA, (b) SiPW-8, and (c) SBA-15.

IR Spectra

The infrared spectra of the samples are shown in Figure 5. It is well known that the Keggin structure of HPMo is composed of one PO₄ tetrahedron surrounded by four tri-metal groups of three edge-sharing MoO₆ octahedra and that HPMo gives several strong typical IR bands at ca. 1062 cm⁻¹ (stretching frequency of P–O in the central tetrahedron PO₄), 963 cm⁻¹ (terminal bands of Mo=O in the exterior octahedron MoO₆), 871, and 793 cm⁻¹ (Mo–O_b–Mo and Mo–O_c–Mo bridge band, respectively) (Figure 5a).^[14] It has been widely reported that pure mesoporous silica of SBA-15 shows the framework bands at about 800 cm⁻¹ (symmetric stretching of Si–O–Si), 960 cm⁻¹ (stretching of Si–O–H), and 1030–1250 cm⁻¹ (*anti*-symmetric stretching of Si–O–Si) (Figure 5c).^[23,25] In our case, SiPMo-8 gives three intense bands at 1098, 961, 803 cm⁻¹, and one shoulder band at 896 cm⁻¹ over 600–1400 cm⁻¹ regions (Figure 5b). It should be noted that some bands of HPMo in the region partially or fully overlapped with the bands of SBA-15, because of the strong contrast between the weak signals of HPMo in the framework of SiPMo-8 and the very strong signals of SBA-15. Three strong bands in the IR spectrum of SiPMo-8 appeared at 803, 961, and 1098 cm⁻¹, from the overlapping of the IR absorption bands of SBA-15 around 800, 960, and 1100 cm⁻¹, and those of HPMo at 793, 963, and 1062 cm⁻¹, respectively. Consequently, the Keggin unit could only be characterized by the stretching modes assigned to bridging bonds: a very low-intensity peak at about 896 cm⁻¹, with slightly shifted shoulder signals, may confirm that the Keggin structure of HPMo encapsulated into the framework of SBA-15 was slightly influenced during the synthesis procedure, in other words, this may indirectly prove that there are interactions

between the silicon species and the heteropolyanion in the framework of SiPMo-8, it can thus be deemed that the Keggin structure of HPMo is preserved in the framework of SiPMo-8.^[14]

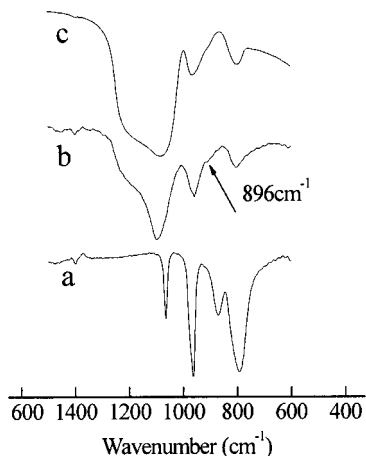


Figure 5. IR spectra of samples: (a) HPMo, (b) SiPMo-8, and (c) SBA-15.

UV/Visible Diffuse Reflectance Spectra

The incorporation of HPMo into the framework of SBA-15 was further indirectly verified by UV/Visible spectra. The UV/Visible spectra of the samples are shown in Figure 6. Bulk HPMo (Figure 6a) shows a broad and strong UV absorption in the range of 200–300 nm, with a maximum centered at about 260 nm, which is a characteristic peak attributed to the oxygen–molybdenum charge-transfer absorption band for Keggin anions. The UV irradiation of the polyoxomolybdate cluster results in charge-transfer from an O²⁻ ion to a Mo⁶⁺ ion, and this occurs at Mo–O–Mo bonds corresponding to the formation of a pair consisting of a hole center (O⁻) and a trapped electron center (Mo⁵⁺). The process can be described as follows:^[14]

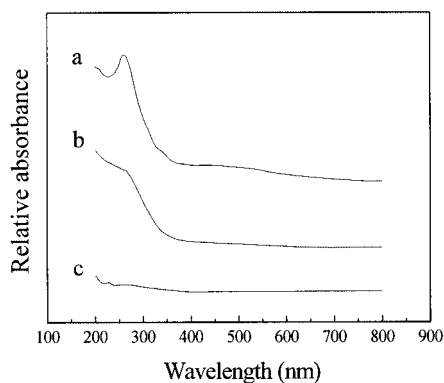
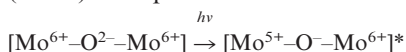


Figure 6. UV/Visible spectra of samples: (a) HPMo, (b) SiPMo-8, and (c) SBA-15.

SBA-15 did not show any signals in the wavelength region studied (Figure 6c). In our case, the SiPMo-8 (Figure 6b) sample has a broad UV absorption in the range

200–300 nm, with a characteristic peak centered at about 260 nm in the spectrum, similar to that of the [PMo₁₂O₄₀]³⁻ species. These results indicate that the primary Keggin structure of HPMo has been introduced into the framework of the mesostructure and is very stable even after the extraction of surfactants and washing with deionized water, which is in agreement with IR results. Similar results can also be observed with ³¹P MAS NMR measurements.

³¹P MAS NMR Spectra

The ³¹P MAS NMR spectra of bulk HPMo and SiPMo-8 are shown in Figure 7. It is well known that the ³¹P MAS NMR chemical shift of bulk HPMo is strongly dependent on the number of crystallized water molecules, in our case bulk HPMo exhibits an intense and sharp line at a chemical shift of around -4.5 ppm in the ³¹P MAS NMR spectrum (Figure 7b) pointing to a uniform phosphorus environment in the structure of HPMo. The ³¹P MAS NMR spectrum of SiPMo-8 also shows an intense and sharp line at around -4.5 ppm and two low intense down-field and up-field chemical shifts (-5.1 and -3.8 ppm, respectively) are observed (Figure 7a). These could be deemed to represent very strong interactions between the molybdophosphoric anions and the framework of SBA-15, which is made up of a network of SiO₂, and could also be attributed to a significant distortion of the heteropoly anion symmetry, whereby the long-range order created by water molecules in the hydrated state of HPMo is lost because of strong chemical interactions between molybdophosphoric anions and the framework of SBA-15. It can be concluded that the Keggin unit (primary structure) is preserved after being incorporated into the framework of SBA-15, because HPMo microcrystallites deposited on the silica surface and heteropoly anions interacting with Si–OH groups have been observed when HPMo was supported on silica.^[14]

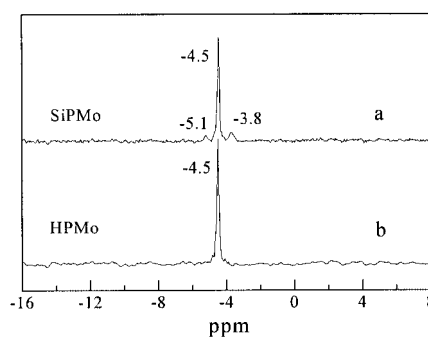


Figure 7. ³¹P MAS NMR spectra of samples: (a) SiPMo-8 and (b) HPMo.

Catalytic Results

1,3,5-Triisopropylbenzene (TIPB) Cracking

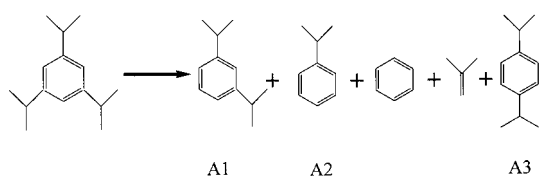
In the reaction of TIPB cracking (see Scheme 1), as shown in Table 2, SBA-15 shows very low catalytic activity (conversion at 2.2%), and HPMo supported on the surface

Table 2. Catalytic activity of SBA-15, HPMo, SiPMo-X, HPMo/SBA, and HPW, SiPW-X, HPW/SBA.

Samples	Conversion of TIPB [wt.-%]	Conversion of esterification ^[a] [wt.-%]		TOF of esterification ^[d] [h ⁻¹]	Conversion of hydroxylation ^[b] [wt.-%]		TOF of hydroxylation ^[e] [h ⁻¹]	Selectivity of hydroxylation ^[f] [wt.-%]		
		Fresh	Reused ^[c]		Fresh	Reused ^[c]		C1	C2	C3
SiPMo-8	50.6	10.2	9.9	3.1	26.5	26.2	251.3	83.4	11.7	4.9
HPMo/SBA	17.4	4.8	0.5	1.5	21.2	4.9	206.6	64.5	28.3	7.2
HPMo	34.3	8.6	–	–	28.7	–	–	41.1	45.5	13.4
SBA-15	2.2	–	–	–	–	–	–	–	–	–
SiPW-8	61.3	12.4	12.2	4.0	17.9	17.6	180.2	89.2	9.5	1.3
HPW/SBA	18.8	6.9	0.7	2.2	15.8	3.0	113.0	72.3	19.3	8.4
HPW	42.6	18.1	–	–	16.6	–	–	50.7	38.8	10.5

[a] Esterification reactions of benzoic acid with *tert*-butyl alcohol. [b] 2,3,6-Trimethylphenol hydroxylation with H₂O₂, acetonitrile as the solvent (polar solvent), 2,3,6-trimethylphenol/H₂O₂ = 3 (molar ratio); catalyst/2,3,6-trimethylphenol ≈ 0.05 (weight ratio), temperature: 353 K, reaction time: 2 h. The products are trimethylhydroquinone (C1, TMHQ), trimethylbenzoquinone (C2, TMBQ), others (C3). Conversion = 2,3,6-trimethylphenol converted to TMHQ, TMBQ and other products/2,3,6-trimethylphenol added in the system. [c] The catalysts were reused five times. [d] Turnover frequency of esterification is moles of *tert*-butyl benzoate yield per mol active site on the surface of the catalyst per hour, using the fresh catalysts. [e] Turnover frequency of hydroxylation is moles of 2,3,6-trimethylphenol converted per mol active site on the surface of the catalyst per hour, using the fresh catalysts. The active site numbers on the surface of SiPMo-8, SiPW-8, HPMo/SBA, and HPW/SBA were estimated on the basis of the amount of HPAs (moles) estimated by ICP analysis, and the surface areas were determined by N₂ adsorption methods. [f] The selectivity of hydroxylation is that of 2,3,6-trimethylphenol hydroxylation with H₂O₂ using the fresh catalysts.

of SBA-15 with impregnation methods gives reaction conversion at 17.4%. In our case, SiPMo-8 shows high catalytic activity and gives reaction conversion at 50.6%, which is higher than that of HPMo/SBA, and the results suggest the potential use of SiPMo-8 as a catalyst for bulky molecule catalytic reactions. Similar phenomena have also been observed when using SiPW-8 and HPW/SBA samples as the catalyst, giving conversion at 61.3 and 18.8%, respectively. We can see that the activity of SiPW-8 in TIPB cracking is higher than that of SiPMo-8, the activity of HPW/SBA is higher than that of HPMo/SBA, and the activity of HPW is also higher than that of HPMo. It is well known that HPW is a stronger acid than HPMo, and TIPB cracking is a typical acidic catalytic reaction, so it is easy to understand the above results.^[17]

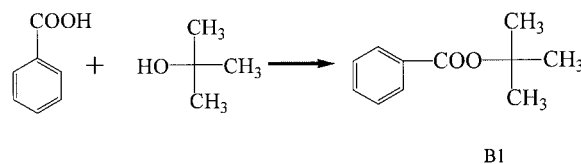


Scheme 1. Catalytic cracking of 1,3,5-triisopropylbenzene (TIPB): [A1] 1,3-diisopropylbenzene; [A2] cumene; [A3] 1,4-diisopropylbenzene.

Esterification of Benzoic Acid with *tert*-Butyl Alcohol

In esterification (see Scheme 2), as shown in Table 2, the SiPMo-8 sample gives conversion at 10.2% (TOF at 3.1 h⁻¹), HPMo/SBA prepared by the impregnation method shows very low catalytic activity (conversion at 4.8%, TOF at 1.5 h⁻¹) compared with the SiPMo-8 sample; the SiPW-8 sample gives conversion at 12.4% (TOF at 4.0 h⁻¹) and HPW/SBA prepared by the impregnation method shows conversion at 6.9% (TOF at 2.2 h⁻¹). Moreover, the SiPMo-8 and SiPW-8 samples still showed similar catalytic activity compared with the corresponding fresh catalysts after the

catalysts were reused five times (Table 2), whereas the conversions with HPMo/SBA and HPW/SBA were reduced remarkably after the catalysts were used five times, to only 0.5 and 0.7%, respectively, which may be attributed to the leaching of the HPAs supported on the surface of SBA-15 during the reactions.^[23,25] The above results suggest that SiPMo-8 and SiPW-8 are very stable in liquid reactions even when they are reused many times, and the leaching of HPAs is hardly observed, as compared with samples prepared by the impregnation method.^[18] Similar phenomena can also be observed in the hydroxylation of 2,3,6-trimethylphenol with H₂O₂.



Scheme 2. Esterification of benzoic acid with *tert*-butyl alcohol: [B1] *tert*-butyl benzoate.

Hydroxylation of 2,3,6-Trimethylphenol with H₂O₂

In hydroxylation (see Scheme 3),^[41] also as shown in Table 2, SiPMo-8 gives conversion at 26.5% (TOF at 251.3 h⁻¹), and HPMo/SBA prepared by the impregnation method shows similar catalytic activity (conversion at 21.2%, TOF at 206.6 h⁻¹). SiPW-8 gives conversion at 17.9% (TOF at 180.2 h⁻¹), HPW/SBA shows similar catalytic activity (conversion at 15.8%, TOF at 113.0 h⁻¹). Moreover, after the catalysts were reused five times (Table 2), SiPMo-8 and SiPW-8 still showed similar catalytic activities (26.2 and 17.6%, respectively) compared with the corresponding fresh catalysts (26.5 and 17.9%, respectively), whereas the conversions with HPMo/SBA and HPW/SBA were reduced remarkably, to only 4.9 and 3.0%, respectively, after the catalysts were recycled five times.

measurements, the volume of adsorbed N₂ was normalized to standard temperature and pressure, specific surface areas were determined from the linear part of the BET equation, the average pore diameter was calculated by using the adsorption branches of the N₂ isotherms. Infrared (IR) spectroscopy was performed with a Bruker IFS 66v/S infrared spectrometer in the range 400–4000 cm⁻¹ by using KBr pellets in vacuo (<0.4 Pa) at ambient temperature. The diffuse reflectance UV/Visible spectra for powder samples were obtained with a Perkin–Elmer Lambda 20 UV/Visible spectrometer equipped with an integrating sphere, and BaSO₄ was used as the internal standard. Solid-state ³¹P magic angle spinning nuclear magnetic resonance (MAS NMR) spectroscopy was performed with an Infinity Plus-400 spectrometer equipped with MAS at a frequency of 104.26 MHz, chemical shifts were referenced to 85% H₃PO₄ as an external standard.

Catalytic Test

Catalytic Cracking of 1,3,5-Triisopropylbenzene

Catalytic cracking of 1,3,5-triisopropylbenzene was carried out by using the pulse technique in a microreactor, and the analyses of the catalytic products were performed by a gas chromatograph (GC-17A, Shimadzu Co.) equipped with a flame ionization detector (FID) with a flexible, 30-m OV-17 quartz capillary column. The catalytic cracking was performed under the following standard conditions: the reaction temperature was 250 °C (no thermal cracking); the reaction pressure was atmospheric pressure; the mass of the catalyst was 0.050 g; 0.2 μL of TIPB was injected for each test; nitrogen was used as the carrier gas at a flow rate of 45 mL/min.

Esterification of Benzoic Acid with *tert*-Butyl alcohol

The esterification of benzoic acid with *tert*-butyl alcohol was performed under nitrogen at 80 °C in a flask (30 mL) containing suspended catalyst powder (60 mesh pass), benzoic acid (5 mmol), and *tert*-butyl alcohol (10 mmol). The amount of catalyst used was 0.150 g. After vigorous agitation for 4 h, the products were analyzed with a gas chromatograph (6890N, Agilent Co.) equipped with a flame ionization detector (FID) with a flexible, 30-m HP-5 quartz capillary column.

Hydroxylation of 2,3,6-Trimethylphenol with H₂O₂

The hydroxylation reaction of 2,3,6-trimethylphenol with H₂O₂ was performed at 80 °C in a flask (50 mL) containing suspended catalyst powder (0.150 g, 60 mesh pass), acetonitrile (5 mL) as the solvent, 2,3,6-trimethylphenol (0.156 mol), and H₂O₂ (0.052 mol), all added at the same time followed by vigorous agitation for 2 h. The products were analyzed with a gas chromatograph (6890N, Agilent Co.) equipped with a flame ionization detector (FID) with a flexible, 30-m INNOWAX quartz capillary column.

Acknowledgments

We are grateful for the financial support of the State Basic Research Project (G2000077507) and the National Natural Science Foundation of China (Grant No. 20101004).

- [1] A. Taguchi, F. Schüth, *Microporous Mesoporous Mater.* **2005**, *77*, 1–45.
- [2] J. A. Rabo, *Appl. Catal., A* **2002**, *229*, 7–10.
- [3] S. Damyanova, L. Dimitrov, R. Mariscal, J. Fierro, L. Petrov, I. Sobrados, *Appl. Catal., A* **2003**, *256*, 183–197.
- [4] J. Haber, K. Pamin, L. Matachowski, D. Mucha, *Appl. Catal., A* **2003**, *256*, 141–151.

- [5] I. V. Kozhevnikov, *Appl. Catal., A* **2003**, *256*, 3–18.
- [6] I. V. Kozhevnikov, *Catal. Rev. - Sci. Eng.* **1995**, *29*, 311–352.
- [7] M. N. Timofeeva, *Appl. Catal., A* **2003**, *256*, 19–35.
- [8] T. Okuhara, *Appl. Catal., A* **2003**, *256*, 213–224.
- [9] M. Misono, *Chem. Commun.* **2001**, 1141–1152.
- [10] Y. Guo, C. Hu, C. Jiang, Y. Yang, S. Jiang, X. Li, E. Wang, *J. Catal.* **2003**, *217*, 141–151.
- [11] P. A. Jalil, M. A. Al-Daous, A. A. Al-Arfaj, A. M. Al-Amer, J. Beltrami, S. A. I. Barri, *Appl. Catal., A* **2001**, *207*, 159–171.
- [12] L. R. Pizzio, P. G. Vázquez, C. V. Cáceres, M. N. Blanco, *Appl. Catal., A* **2003**, *256*, 125–139.
- [13] S. Mukai, T. Sugiyama, H. Tamon, *Appl. Catal., A* **2003**, *256*, 99–105.
- [14] S. Damyanova, L. Dimitrov, R. Mariscal, J. Fierro, L. Petrov, I. Sobrados, *Appl. Catal., A* **2003**, *256*, 183–197.
- [15] A. Bielanski, A. Lubanska, J. Pozniczek, A. Micek-Ilnicka, *Appl. Catal., A* **2003**, *256*, 153–171.
- [16] H. Kosslick, G. Lischike, B. Parlitz, W. Storek, R. Fricke, *Appl. Catal., A* **1999**, *184*, 49–60.
- [17] A. Ghanbari-Siahkali, A. Philippou, J. Dwyer, M. Anderson, *Appl. Catal., A* **2000**, *192*, 57–69.
- [18] Y. Izumi, K. Hisano, T. Hida, *Appl. Catal., A* **1999**, *181*, 277–282.
- [19] R. L. Augustine, S. K. Tanielyan, N. Mahata, Y. Gao, A. Zsigmond, H. Yang, *Appl. Catal., A* **2003**, *256*, 69–76.
- [20] H. Li, N. Perkas, Q. Li, Y. Gofer, Y. Koltypin, A. Gedanken, *Langmuir* **2003**, *19*, 10409–10413.
- [21] Y. Guo, Y. Wang, C. Hu, Y. Wang, E. Wang, *Chem. Mater.* **2000**, *12*, 3501–3508.
- [22] K. Nowińska, R. Fórmaniak, W. Kaleta, A. Waclaw, *Appl. Catal., A* **2003**, *256*, 115–123.
- [23] C. Shi, R. Wang, G. Zhu, S. Qiu, J. Long, *Eur. J. Inorg. Chem.* **2005**, 4801–4807.
- [24] Q. Liu, W. Wu, J. Wang, X. Ren, Y. Wang, *Microporous Mesoporous Mater.* **2004**, *76*, 51–60.
- [25] C. Shi, M. Xin, R. Wang, Y. Xie, L. Hu, L. Xu, R. Zhang, G. Zhu, S. Qiu, *Chem. J. Chin. Univ.* **2005**, *26*, 1198–1201.
- [26] L. Yang, Y. Qi, X. Yuan, J. Shen, J. Kim, *J. Mol. Catal. A* **2005**, *229*, 199–205.
- [27] H. Yun, M. Kuwabara, H. Zhou, I. Honma, *J. Mater. Sci.* **2004**, *39*, 2341–2347.
- [28] P. M. Rao, A. Wolfson, S. Kababya, S. Vega, M. V. Landau, *J. Catal.* **2005**, *232*, 210–225.
- [29] C. T. Kresge, M. E. Leonowicz, W. J. Roth, J. C. Vartuli, J. S. Beck, *Nature* **1992**, *359*, 710–712.
- [30] S. S. Kim, W. Zhang, T. J. Pinnavaia, *Science* **1998**, *282*, 1302–1305.
- [31] D. Zhao, J. Feng, Q. Huo, N. Melosh, G. H. Fredrickson, B. F. Chmelka, G. D. Stucky, *Science* **1998**, *279*, 548–552.
- [32] A. Corma, *Chem. Rev.* **1997**, *97*, 2373–2419.
- [33] Y. Liu, Y. Cao, N. Yi, W. Feng, W. Dai, S. Yan, H. He, K. Fan, *J. Catal.* **2004**, *224*, 417–428.
- [34] A. Corma, A. Martinez, V. Martinez-Soria, *J. Catal.* **1997**, *169*, 480–494.
- [35] T. Blasco, A. Corma, A. Martinez, P. Martinez-Escolano, *J. Catal.* **1998**, *177*, 306–313.
- [36] Q.-H. Xia, K. Hidajat, S. Kawi, *J. Catal.* **2002**, *209*, 433–444.
- [37] Q.-H. Xia, K. Hidajat, S. Kawi, *J. Catal.* **2002**, *205*, 318–331.
- [38] B. Bachiller-Baeza, J. A. Anderson, *J. Catal.* **2002**, *212*, 231–239.
- [39] Q.-H. Xia, K. Hidajat, S. Kawi, *Catal. Today* **2001**, *68*, 255–262.
- [40] P. M. Rao, M. V. Landau, A. Wolfson, A. M. S.-T. M. Herskowitz, *Microporous Mesoporous Mater.* **2005**, *80*, 43–55.
- [41] X. Meng, Z. Sun, S. Lin, M. Yang, X. Yang, J. Sun, D. Jiang, F. Xiao, *Appl. Catal., A* **2002**, *236*, 17–22.

Received: March 3, 2006

Published Online: June 19, 2006